DALTON

Ten-vertex polyhedral monoheteroborane chemistry: syntheses, molecular structures, and nuclear magnetic resonance characterization of some 9-substituted 6-aza- and 6-thia-*arachno*-decaboranes

Bohumil Štíbr,[a,b] Josef Holub,[a] Tomáš Jelínek,[a,b] Xavier L. R. Fontaine,[b] Jiři Fusek,[a] John D. Kennedy[b] and Mark Thornton-Pett[b]

[a] *The Institute of Inorganic Chemistry of the Academy of Sciences of the Czech Republic, 250 68 Rez, The Czech Republic*

[b] *The School of Chemistry, University of Leeds, Leeds LS2 9JT, UK*

Reactions between *nido*-NB_9H_{12} **1** or *nido*-SB_9H_{11} **2** and Lewis bases L under a variety of conditions gave two series of corresponding *arachno* compounds, *exo*-9-L-*arachno*-6-NB_9H_{12} **3** and *exo*-9-L-*arachno*-6-SB_9H_{11} **4** where L include NEt_3, quinoline, isoquinoline, pyridine, urotropine (uro), MeCN, MeNC, PPh_3, NH_3 and SMe_2. All these compounds were characterized by mass spectrometry together with ^{11}B and ^1H NMR spectroscopy. In some cases, the *endo* analogues *endo*-9-L-*arachno*-6-EB_9H_{11}, where E = NH **5** or S **6** have also been tentatively identified by NMR spectroscopy. Single-crystal X-ray diffraction studies have been carried out on an example of **3** (L = MeNC) and two examples of **4** (L = $\frac{1}{2}$ uro or MeNC).

In our two laboratories there is a continuing and developing interest in the synthesis, NMR properties, structural characterization, and reactions of the Group 15 and 16 polyhedral heteroboranes,[1] with special emphases thus far on the azaborane[1-7] and thiaborane[4,7-14] families. In these areas, we have reported on *arachno*-4-NB_8H_{13},[2,4] 7-L-*arachno*-4-NB_8H_{11} {L = H^-, pyridine (py), quinoline (quin), isoquinoline (iquin), urotropine (1,3,5,7-tetraazatricyclo[3.3.1.1^{3,7}]decane) (uro) or MeCN},[7] *nido*-6-NB_9H_{12},[3,4] 9-L-*arachno*-6-NB_9H_{12} (L = H, SMe_2, MeCN or PPh_3),[3,4] *arachno*-6,9-$N_2B_8H_{12}$,[5] *arachno*-4-SB_8H_{12},[4,8,9,13] 7-L-*arachno*-SB_8H_{12} (L = H^-, SMe_2, MeCN or PPh_3),[14] *nido*-6-SB_9H_{11}[10] and the [*arachno*-6-SB_9H_{12}]$^-$ anion.[10,11] The ten-vertex monoheteroboranes *nido*-6-NB_9H_{12} **1**[3,4,15,16] and *nido*-6-SB_9H_{11} **2**[17-19] and some examples of those in the corresponding ten-vertex *arachno* categories *exo*-9-L-*arachno*-6-NB_9H_{12} **3** and *exo*-9-L-*arachno*-6-S_9H_{11} **4** have been known for some time, and have been reported with varying degrees of structural characterization. Known species in the *arachno*-azaborane category **3** include examples where L = H^-, SMe_2, MeCN, Bu^{t}NC, *cyclo*-$C_6H_{11}NC$, or pyridine (py),[3,4,15] and those in the *arachno*-thiaborane category **4** include examples where L = H^-, SMe_2, OH^-, NEt_3, MeCN, Me_2NCHO, tetrahydrofuran (thf), (Bu^t)-MeCHNH$_2$, PPh_3 or μ_2-(4,*exo*-9)-$Me_3SiNNNH$].[11,17,20-25] Of these, one *arachno*-NB_9 species and three *arachno*-SB_9 species, namely *exo*-9-(*cyclo*-$C_6H_{11}NC$)-6-NB_9H_{12},[15] the [*arachno*-6-SB_9H_{12}]$^-$ anion,[11,21] *exo*-9-(NEt_3)-6-SB_9H_{11},[23] and [μ_2-(4,*exo*-9)-$Me_3SiNNNH$]-*arachno*-6-SB_9H_{10},[24] have been characterized by X-ray diffraction studies that have confirmed the general *arachno* ten-vertex cluster configurations as in schematic structures **3** and **4**.

In addition to these, some less stable thiaboranes of the *endo*-9-L-*arachno*-6-SB_9H_{12} constitution **5** have been detected by NMR spectroscopy, for example where L is an alkylisocyanide,[15] and two stable compounds of this structural type have been isolated, for L = OH^-[10,26] and for L = HN=C-(Bu^t)Me,[25] the last having been structurally characterized by X-ray diffraction work. The aim of the work described in this paper is to develop the chemistry of compounds of type **3** and **4** by the preparation of a more extended series to further our examination for coherent systematics of NMR and structural behaviour in isoelectronic and isostructural series of polyhedral boron-containing compounds.

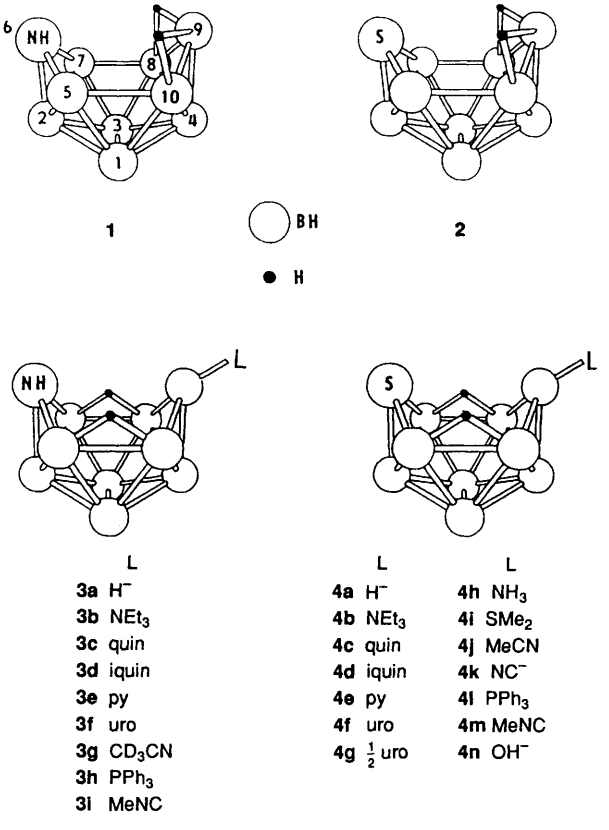

Experimental

General

Unless otherwise stated, all reactions were carried out under dry dinitrogen, although some subsequent operations, *e.g.* analytical thin-layer chromatography (TLC) and preparative TLC, were

Table 1 Properties of the products from reactions between *nido*-6-NB_9H_{12} and Lewis bases in dichloromethane

Reaction conditions			Products				
Base	Ratio[a]	*t*/h	Product(s)	Yield(%)	Colour	R_f	m/z_{max}
NEt_3	2:1	4	**3b**	93	White	0.40[b]	192
			5b[c]	*ca.* 3	White	0.54[b]	—
quin	2:1	3	**3c**	87	Yellow	0.26[d]	254
iquin	2:1	3	**3d**	78	Yellow	0.27[b]	254
py	2:1	3	**3e**	82	Yellow	0.16[d]	204
uro	1.5:1	4	**3f**	53	White	0.23[e]	265
CD_3CN[f]	Excess	1	**3g**[g]	80[g]	White	—	125
			5g[g]	*ca.* 20[g]	White	—	—
PPh_3	1.5:1	3	**3h**	45	White	0.28[d]	125
MeNC	2:1	10	**3i**	0.30	White	0.30[b]	166

[a] Molar ratio base: NB_9H_{12}; 9-(MeCN)-*arachno*-6-NB_9H_{12} may also be employed as a starting material. [b] 30% Hexane in CH_2Cl_2. [c] Rapid conversion into compound **3b** during the NMR experiment. [d] 50% Hexane in CH_2Cl_2. [e] 20% MeCN in CH_2Cl_2. [f] Reaction carried out in an NMR tube with an excess of CD_3CN without solvent. [g] NMR-tube experiment; possible initial equilibrium established among compounds **1**, MeNC, **5b** and **3g**, with NB_8H_{13} then being slowly formed (initial molar ratio *ca.* 1:1:0.8); the mixture contained *ca.* 90% of NB_8H_{13} after 24 h.

carried out in air. Methyl isocyanide,[28] and the starting heteroboranes *nido*-6-NB_9H_{12} **1** and *nido*-6-SB_9H_{11} **2**,[16,19] were prepared by literature methods. Hexane and dichloromethane were distilled from calcium hydride, chloroform and acetonitrile from P_4O_{10}, dimethyl sulfide from solid potassium hydroxide, and tetrahydrofuran from sodium diphenylketyl prior to use. Other compounds and solvents were of reagent or analytical grade and were used as purchased. All evaporations of solvents were carried out using standard rotary-evaporation techniques and vacuum filtrations were performed using a standard Schlenk apparatus. Preparative TLC was carried out using silica gel (Fluka, type GF 254) as the stationary phase on plates of dimensions 200 × 200 × 1 mm, made on glass formers from aqueous slurries followed by drying in air at 80 °C. The purity of individual chromatographic fractions was checked by analytical TLC on Silufol (Kavalier, silica gel on aluminium foil; detection by diiodine vapour, followed by 2% aqueous $AgNO_3$ spray).

Physical measurements

Low-resolution mass spectra were obtained using a JEOL HP-5985 or a VG AutoSpec instrument [70 eV (1.12×10^{-17} J) electron impact (EI) ionization], and proton (^1H) and boron (^{11}B) NMR spectroscopy was carried out at 2.35, 9.4 and 11.75 T on JEOL FX100, Bruker AM 400, and Varian XL-500 instruments, respectively. The [^{11}B–^{11}B] correlation spectroscopy (COSY) and ^1H-{^{11}B(selective)} NMR experiments were essentially as described in other recent papers from our laboratories.[29,30] Chemical shifts are given in ppm to high frequency (low field) of Ξ = 32.083 971 MHz (nominally $F_3B{\cdot}OEt_2$ in $CDCl_3$) for ^{11}B (quoted ± 0.5 ppm) and Ξ = 100 MHz ($SiMe_4$) for ^1H (quoted ± 0.05 ppm), Ξ being defined as in ref. 31. Solvent resonances were used as internal secondary standards. Coupling constants $^1J(^{11}B$–$^1H)$ were taken from resolution-enhanced ^{11}B spectra with digital resolution 8 Hz and are given in Hz.

Syntheses

Tetrabutylammonium tridecahydro-6-aza-*arachno*-decaborate(1−) 3a. To a solution of *nido*-6-NB_9H_{12} **1** (124 mg, 1 mmol) in thf (10 cm^3) was added $Na[BH_4]$ (76 mg, 2 mmol) and the mixture heated at reflux for 4 h. Water (20 cm^3) was added, the thf was evaporated and the remaining aqueous solution precipitated by the addition of solid $[NBu_4]Cl$ (278 mg, 1 mmol) with shaking. The white precipitate was filtered off, washed with water (10 cm^3), and dried *in vacuo* to yield $[NBu_4][$*arachno*-6-$NB_9H_{13}]$ **3a** (320 mg, 86%), which was identified by comparison with the literature data[3,4,9] and by NMR spectroscopy (Table 8).

General synthesis of 9-substituted 6-aza-*arachno*-decaboranes 3 and 6-thia-*arachno*-decaboranes 4. In a typical experiment, a mixture of *nido*-6-NB_9H_{12} **1** or *nido*-6-SB_9H_{11} **2** (1 mmol) and an excess of Lewis base [see Table 1 (for E = NH) and Table 2 (for E = S)] was dissolved in dichloromethane (10 cm^3) and was left to stand for 1–10 h (see Tables 1 and 2) at ambient temperature (dihydrogen evolution). The volatile components were then evaporated and the solid residue subjected to preparative TLC on silica gel, using solvents as in Tables 1 and 2 as the liquid phase. The main fractions, of R_f as in Tables 1 and 2, were collected, evaporated to dryness and crystallized from a concentrated solution in dichloromethane that was overlayered by a two-fold amount of hexane. This procedure yielded crystals (for yields see Tables 1 and 2) which were identified as the *exo*-9-L-*arachno*-6-EB_9H_{11} compounds **3a**–**3i** and **4a**–**4j**, **4l** and **4m** by NMR spectroscopy, mass spectrometry and X-ray crystallography as described below. Analytical products were obtained by repeated crystallizations. For other characteristics of individual compounds see Tables 1 and 2. In the thiaborane systems with L = quin and MeNC, cluster-degradation products of the general formula *exo*-L-*arachno*-4-SB_8H_{10} are isolatable from the faster-moving chromatographic fractions, as reported earlier.[14] The thiaborane experiment with MeCN was also carried out *in situ* in an NMR tube and followed by NMR spectroscopy without the isolation of individual components (see Results and Discussion section).

Undecahydro-*exo*-9-isocyano-6-thia-*arachno*-decaborate(1−) 4k and 8-trimethylamine-7-thia-8-carba-*nido*-undecaborane(9) 8b. Solid sodium cyanide (2.8 g, 40 mmol) was added to a solution of *nido*-6-SB_9H_{11} **2** (2.84 g, 20 mmol) in thf (50 cm^3) and the mixture was stirred for 8 h at room temperature. The excess of cyanide was then filtered off and the thf evaporated from the filtrate. The solid residue was dissolved in water (50 cm^3), the solution filtered with charcoal (*ca.* 1 g), and the clear yellowish filtrate acidified (intensive cooling to *ca.* 0 °C) with concentrated hydrochloric acid to pH *ca.* 1. The mixture was then extracted with diethyl ether (2 × 50 cm^3), the ether layer separated, and the ether removed by evaporation after the addition of water (50 cm^3). The resulting aqueous solution was filtered with charcoal, neutralized by 10% NaOH to pH *ca.* 8, and treated with dimethyl sulfate (5 cm^3, dropwise) with intensive shaking and cooling to *ca.* 10 °C. The white precipitate

Table 2 Properties of the products from reactions between *nido*-6-SB_9H_{11} and Lewis bases in dichloromethane

Reaction conditions			Products				
Base	Ratio[a]	*t*/h	Product(s)	Yield(%)	Colour	R_f	m/z_{max}
NEt_3	2:1	4	**4b**	63	White	0.29[b]	243
quin	2:1	12	**4c**	63	Yellow	0.28[c]	271
			9a[d]	15	Yellow	0.35[c]	259[d]
iquin	2:1	24	**4d**	18	Yellow	0.32[c]	271
py	1.1:1	24	**4e**	85	Yellow	0.27[e]	221
uro	0.7:1	48	**4f**	36	White	0.08[f]	282
			4g	39	White	0.37[f]	424
NH_3	Excess[g]	2	**4h**	55	White	0.20[h]	159
SMe_2	Excess[i]	24	**4i**	89	White	0.33[c]	204
MeCN	Excess[i]	4	**4j**	40	White	0.30[e]	183
			9b[d]	35	White	0.37[e]	171[d]
PPh_3	1.1:1	24	**4l**	85	White	0.27[e]	404
MeNC	7:1	12	**4m**[d]	32	White	0.24[c]	183
			9c[d]	21[d]	White	0.28[c]	171[d]

[a] Molar ratio base: SB_9H_{11}; compound **4i** may also be employed as a starting material for amine bases. [b] 50% Hexane in CH_2Cl_2. [c] 33% Hexane in benzene. [d] See also ref. 14. [e] In benzene. [f] In CH_2Cl_2. [g] Gaseous NH_3 bubbled through a CH_2Cl_2 solution. [h] 10% MeCN in CH_2Cl_2. [i] Carried out in the absence of CH_2Cl_2.

thus formed was filtered off, dried *in vacuo* and recrystallized from a concentrated dichloromethane solution that was overlayered by the same volume of hexane to give 8-(NMe_3)-*nido*-7,8-SCB_9H_9 **8b** (0.8 g, 18%), m.p. 321–323 °C (lit.,[27] 334–336 °C), *m*/*z* 211 (M^+, 15%); $\delta(^{11}B)$ ($CDCl_3$) −7.5 [1 B, *J*(BH) 153, B(2)], −10.2 [1 B, *J*(BH) *ca.* 127, B(9)], −12.8 [2 B, *J*(BH) *ca.* 170, B(4, 11)], −14.3 [1 B, *J*(BH) *ca.* 175, B(6)], −16.7 [1 B, B(10)], −18.7 [1 B, B(5)], −19.1 [1 B, *J*(BH) *ca.* 150, B(3)] and −42.2 [1 B, *J*(BH) 149 Hz, B(1)]; $\delta(^1H)$ ($CDCl_3$) 3.19 (9 H, NMe_3), 2.44 [1 H, H(4)], 2.35 [1 H, H(2)], 2.20 [1 H, H(9)], 2.18 [1 H, H(4 or 11)], 2.04 [1 H, H(3)], 2.02 [1 H, H(5)], 1.73 [1 H, H(6)], 1.45 [1 H, H(10)] and 0.94 [1 H, H(1)]. The aqueous filtrate remaining after the isolation of **8b** was precipitated by 1 mol dm^{-3} aqueous [NMe_4]Cl (10 cm^3) and the white precipitate filtered off, washed with water (20 cm^3), and recrystallized from chloroform–acetonitrile (1:1) to yield [NMe_4][*exo*-9-(NC)-*arachno*-6-SB_9H_{11}]$^-$ **4k** (2.4 g, 50%), R_f ($CHCl_3$–MeCN 2:1) 0.25, which was identified by NMR spectroscopy (Table 9) and comparison with literature data.[27]

Tetraphenylphosphonium 9-*exo*- and 9-*endo*-hydroxyundecahydro-6-thia-*arachno*-decaborates 4n and 6n. A solution of *nido*-6-SB_9H_{11} **2** (141 mg, 1 mmol) in hexane (20 cm^3) was shaken with 10% aqueous KOH (20 cm^3) for 2 h at ambient temperature. The aqueous layer was separated and precipitated with 1 mol dm^{-3} [PPh_4]Cl (1 cm^3). The pale yellow precipitate was filtered off, washed with water (20 cm^3), dried *in vacuo* at ambient temperature, and then subjected to repeated preparative TLC using 33% MeCN in hexane as the liquid phase. This resulted in the separation of two main bands of R_f 0.45 and 0.31, which were isolated by extraction with MeCN and evaporation to dryness. The individual products, [PPh_4]$^+$-[*exo*-9-(HO)-*arachno*-6-SB_9H_{11}]$^-$ **4n** (159 mg, 32%) and [PPh_4]$^+$[*endo*-9-(HO)-*arachno*-6-SB_9H_{11}]$^-$ **6n** (149 mg, 30%), were purified by crystallization from dichloromethane solutions that were overlayered by hexane. They were identified by NMR spectroscopy (see Table 9).

Crystallography

Crystals of *exo*-9-(MeNC)-*arachno*-6-NB_9H_{12} **3i**, *exo*,*exo*′-9,9′-(uro)-(*arachno*-6-SB_9H_{11})$_2$ **4g** and *exo*-9-(MeNC)-*arachno*-6-SB_9H_{11} **4m** suitable for single-crystal X-ray diffraction studies were obtained as described in the preceding paragraphs. The data set for **4g** was corrected for absorption using azimuthal ψ-scans (maximum and minimum transmission factors 0.7122 and 1.0000). All crystallographic measurements were made at 200 K on a Stoe STADI-4 diffractometer operating in the ω–θ scan mode and, for **3i** and **4g**, an on-line profile-fitting method.[32] Full details of crystal data, data collection and structure solution and refinement are given in Table 3.

The structures of all three compounds were solved by direct methods using SHELXS 86.[33] Both **3i** and **4m** were found to possess crystallographic C_s symmetry with the mirror plane passing through atoms B(4), B(2), N(6) or S(6) and the non-hydrogen atoms of the MeNC substituent. Refinement, by full-matrix least squares using SHELX 76,[34] was essentially the same for all three compounds. Non-hydrogen atoms were refined with anisotropic displacement parameters, and all hydrogen atoms were located on Fourier-difference syntheses and freely refined with individual isotropic displacement parameters except for the methylene hydrogen atoms of **4g** which were placed in idealized positions and refined with an overall isotropic displacement parameter. The weighting scheme $w = [\sigma^2(F_o) + 0.0002(F_o)^2]^{-1}$ was used in all three cases.

Complete atomic coordinates, thermal parameters and interatomic distances and angles have been deposited at the Cambridge Crystallographic Data Centre. See Instructions for Authors, *J. Chem. Soc., Dalton Trans.*, 1996, Issue 1.

Results and Discussion

Syntheses

In addition to the methods previously reported,[3,4,9,11] we have now found that the parent (*i.e.* unsubstituted) compound of structural category **3**, *i.e.* the [*arachno*-NB_9H_{13}]$^-$ anion **3a**, can also be prepared conveniently in 86% yield by treatment of the *nido*-azaborane NB_9H_{12} **1** with sodium tetrahydroborate in thf at reflux for 4 h. The other compounds **3b**–**3i** (Table 1) and **4b**–**4n** (Table 2) of the general *exo*-9-L-*arachno*-6-EB_9H_{11} constitution (schematic structures **3** and **4**) were prepared essentially according to the previously established reactions[3,4,15,17,24,25] between *nido*-NB_9H_{12} **1** or *nido*-SB_9H_{12} **2** and Lewis bases L [path (*i*) in Scheme 1, where E = NH or S], although with some modifications in detail from published procedures (see Experimental section). Most of the reactions were carried out in the presence of an excess, or of at least 1 equivalent, of the appropriate L, using dichloromethane as solvent. With some weaker liquid bases, such as SMe_2 and MeCN, a large excess of L was used (see Tables 1 and 2) without any other solvent. As in the case of the previously reported nine-vertex thiaboranes *exo*-6-L-*arachno*-4-SB_8H_{10},[14] the

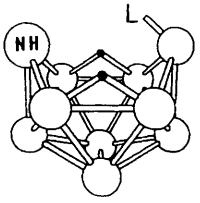

5b NEt_3
5g CD_3CN

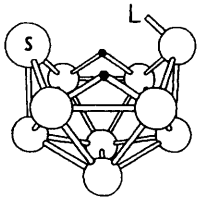

6n OH^-
6b CN^-

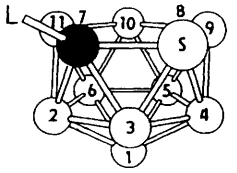

8a NH_3
8b NMe_3

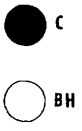

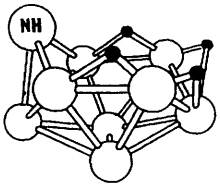

7

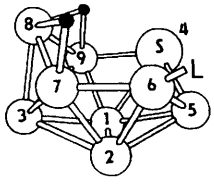

9a quin
9b MeCN
9c MeNC

urotropine reaction also yielded a bidentate bis(polyhedral) compound *exo,exo'*-9,9'-(uro)-(*arachno*-6-SB_9H_{11})$_2$ **4g**, in addition to the monodentate adduct **4f**.

As previously demonstrated, in part, in the reactions between *nido*-SB_9H_{12} **2** and either the cyanide anion or alkyl isocyanides,[27] the formation of the *exo*-ligand compounds of structure type **4** can be accompanied by the formation of *endo*-thiaborane isomers **6** [*e.g.* **6b**, where L = CN^- and E = S, path (*ii*) in Scheme 1],[10,11,22,26] which are mostly unstable and which readily convert into the more stable *exo*-ligand compounds of type **4** [path (*iv*) in Scheme 1]. In the present work we have similarly also observed compounds **6n** (L = OH^-) and **6b** (L = CN^-) in the thiaborane systems.

We have now also observed the formation of unstable *endo*-ligand isomers in the azaborane systems (structure type **5**), specifically in the reactions of *nido*-NB_9H_{12} **1** with NEt_3 or CD_3CN. Thus, in the former case, both the *endo* isomer **5b** and the stable *exo* compound **3b** were isolated by TLC. However, within approximately 2 h during NMR measurements, the ten-vertex *endo* compound **5b** was observed to convert into an approximately 1:1 mixture that consisted of the ten-vertex *exo* isomer **3b** and the nine-vertex azaborane *arachno*-4-NB_8H_{13} **7** [path (*iii*) in Scheme 1, E = NH]. Compound **7** presumably results from cluster degradation by ambient moisture. A similar formation of the ten-vertex *endo*-CD_3CN compound **5g** was observed *in situ* by NMR spectroscopy in the reaction between *nido*-NB_9H_{12} **1** and an excess of CD_3CN in an NMR tube. Here, after 2 h of measurement, there appears to be an equilibrium among the deuteriated MeCN, the *nido* compound **1** (*ca.* 10%), the *endo* compound **5g** (*ca.* 10%), and its *exo*-isomer **3g** (*ca.* 70%), with some degradation to give nine-vertex *arachno*-4-B_8H_{13} **7** (*ca.* 10%). On the other hand, a stable anionic [*endo*-9-(OH)-6-SB_9H_{11}]$^-$ anion **6n** is formed, together with an approximately equal amount of its *exo* isomer **4n** (yields 30 and 32%, respectively), from the reaction between the *nido*-thiaborane **2** and hydroxide ion in a water–hexane mixture, followed by precipitation with $[PPh_4]Cl$ and separation by preparative TLC. The *endo*-substituted anion **6n** has been

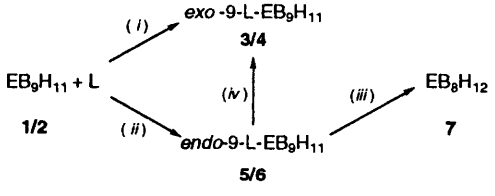

Scheme 1

reported earlier[10] as a product from the air oxidation or hydrolysis of the unsubstituted $[SB_9H_{12}]^-$ anion **4a**, and has also been prepared by the action of aqueous OH^- on the PPh_3 *arachno* compound **4l**.[26]

In the context of these *endo* compounds we find that a modification of the previously reported[27] reaction between *nido*-SB_9H_{11} **2** and the $[CN]^-$ anion in thf solution, followed by methylation with methyl sulfate, results in the formation of the neutral eleven-vertex carbathiaborane 7-(NMe_3)-*nido*-7,8-CSB_9H_9 **8b** (yield 18%), as well as in the isolation of the expected ten-vertex [*exo*-9-(NC)-*arachno*-6-SB_9H_{11}]$^-$ anion **4k** [yield 50%, path (*i*) in Scheme 1]. It seems reasonable here to postulate that the effective intermediate in the formation of the carbathiaborane compound **8b** might be the unstable *endo* isomer **6b**[27] of the [9-(CN)-*arachno*-6-SB_9H_{11}]$^-$ anion [path (*ii*)]. On methyl sulfate treatment this would undergo a carbon-insertion reaction in acidic solution to give the trimethylamine–carbathiaborane adduct **8b** *via* methylation of the presumed amine intermediate **8a** that we have not isolated. Here, on the basis of NMR arguments as discussed below, we may have to consider an isocyano-structure for the anion **4k** as well as the previously reported[27] cyano-arrangement. In contrast to this *Aufbau* process to give an eleven-vertex cluster, we have also observed, in the reactions of the *nido*-thiaborane **2** with quinoline, MeCN and MeNC, some dismantling to form nine-vertex *exo*-6-L-*arachno*-4-SB_8H_{10} species of constitution **9** (specifically compounds **9a**–**9c**) as by-products.[14]

X-Ray diffraction studies

The solid-state molecular structures of *exo*-9-(MeNC)-*arachno*-6-NB_9H_{12} **3i**, *exo,exo'*-9,9'-(uro)-(*arachno*-6-SB_9H_{11})$_2$ **4g** and *exo*-9-(MeNC)-*arachno*-6-SB_9H_{11} **4m** were determined by single-crystal X-ray diffraction analysis and are depicted in Figs. 1, 2 and 3, respectively. Crystal data and structure solution parameters are in Table 3, atomic coordinates in Table 4, cluster interatomic distances in Table 5, selected angles between interatomic vectors for cluster atoms in Table 6, and selected exocluster bond distances and angles in Table 7.

Inspection of the structures shows that each of the three compounds adopts the same symmetric *arachno* configuration (schematic structures **3** and **4**) that has the NH or S heteroatomic unit at the least-connected cluster position (6), and which has a pair of bridging hydrogen atoms localized at the B(7)–B(8) and B(5)–B(10) positions in the open face. In each

Table 3 Crystallograhic data for *exo*-9-(MeNC)-*arachno*-6-NB_9H_{12} **3i**, *exo,exo'*-9,9'-(uro)-(*arachno*-6-SB_9H_{11})$_2$ **4g** and *exo*-9-(MeNC)-*arachno*-6-SB_9H_{11} **4m**

	3i	**4g**	**4m**
Formula	$C_2H_{15}B_9N_2$	$C_6H_{34}B_{18}N_4S_2$	$C_2H_{14}B_9NS$
M	164.45	365.07	181.51
Crystal dimensions/mm	0.8 × 0.5 × 0.4	0.45 × 0.2 × 0.2	0.45 × 0.2 × 0.2
Crystal system	Monoclinic	Monoclinic	Orthorhombic
Space group	$P2_1/m$	$P2_1/a$	*Pnma*
a/pm	592.26(4)	1270.84(6)	1120.74(8)
b/pm	920.53(9)	1118.87(5)	879.51(7)
c/pm	940.73(8)	1660.52(8)	1109.57(7)
β/°	90.237(6)	104.797(1)	
U/nm^3	0.512 88(7)	2.2828(2)	1.0937(2)
Z	2	4	4
D_c/g cm^{-3}	1.06	1.22	1.10
$F(000)$	172	880	370
μ/cm^{-1}	0.48	20.57	2.26
Radiation	Mo-Kα	Cu-Kα	Mo-Kα
λ/pm	71.069	154.184	71.069
Scan width/° + α-doublet splitting	*a*	*a*	1.05
Scan speeds/° min^{-1}	*a*	*a*	1.5–8.0
$2\theta_{min,max}$/°	4.0, 50.0	4.0, 130.0	4.0, 50.0
No. data collected	1257	4111	1151
No. data observed ($\|F_o\| > 4\sigma\|F_o\|$)	1114	3391	930
ρ_{max}, ρ_{min}/e Å^{-3}	0.23, −0.25	0.26, −0.25	0.23, −0.25
Δ/σ_{max}	0.48	0.001	0.41
R^b	0.0400	0.0325	0.0383
R'^c	0.0456	0.0382	0.0465
No. parameters	105	360	102

[a] Scan divided into 30 steps, scan width and step sizes calculated from a learnt profile, scan speeds 0.4–1.5 s per step. [b] $R = \Sigma(|F_o| - |F_c|)/\Sigma|F_o|$. [c] $R' = \Sigma w(|F_o| - |F_c|)^2/\Sigma w|F_o|^2$.

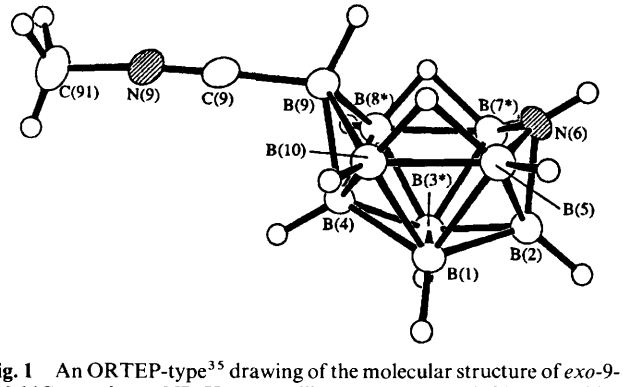

Fig. 1 An ORTEP-type[35] drawing of the molecular structure of *exo*-9-(MeNC)-*arachno*-6-NB_9H_{12} **3i**. Ellipses are at the 50% probability level, whereas hydrogen atoms are drawn as small circles with an arbitrary small radius. Atoms B(2), B(4), B(6), B(9), C(9), N(9) and C(91) are positioned on a crystallographic mirror plane at $y = \frac{1}{4}$ so that the following pairs of atoms are related by the symmetry operator x, $\frac{1}{2} - y$, z: B(1) and B(3*); B(5) and B(8*); B(6) and B(7*)

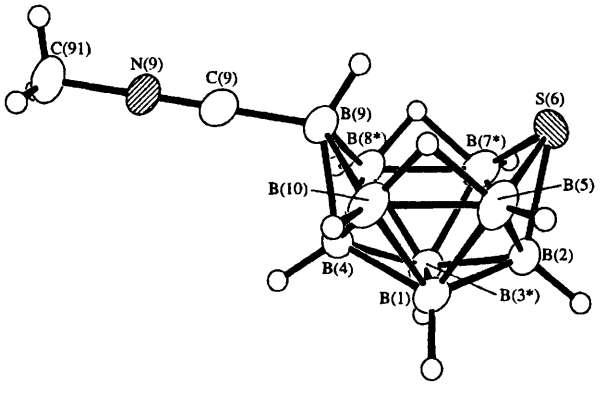

Fig. 3 An ORTEP-type drawing of the molecular structure of *exo*-9-(MeNC)-*arachno*-6-SB_9H_{11} **4m**. Ellipses are at the 50% probability level and hydrogen atoms are drawn as small circles with an arbitrary small radius. Atoms B(2), B(4), B(6), B(9), C(9), S(9) and C(91) are positioned on a crystallographic mirror plane at $y = \frac{1}{4}$ so that the following pairs of atoms are related by the symmetry operator x, $\frac{1}{2} - y$, z: B(1) and B(3*); B(5) and B(8*); B(6) and B(7*)

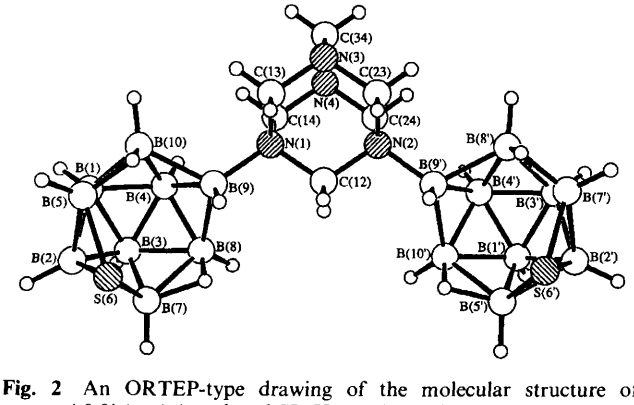

Fig. 2 An ORTEP-type drawing of the molecular structure of *exo,exo'*-9,9'-(uro)-(*arachno*-6-SB_9H_{11})$_2$ **4g**. Ellipses are at the 50% probability level, whereas hydrogen atoms are drawn as small circles with an arbitrary small radius

case the ligand moiety is bound to the B(9) atom in an *exo* fashion. The neutral {B(6)HL} unit is isolobal[29] with an anionic $\{BH_2\}^-$ unit, and hence the clusters of the adduct compounds of types **3** and **4** are formally isoelectronic with the parent anions [*arachno*-6-NB_9H_{13}]$^-$ **3a** and [*arachno*-6-SB_9H_{12}]$^-$ **4a**,[3,4,15,17] and with the binary borane parent $[B_{10}H_{14}]^{2-}$.

Cluster interboron distances are within normal ranges.[37] Detailed intercomparison of equivalent internuclear distances in the clusters of compounds **3i**, **4g** and **4m** in Table 5 reveals marked similarities. Except, of course, for the large differences between equivalent N–B and S–B distances, the only consistently different variations are for the B(2)–B(5) and B(2)–B(7) distances flanking the heteroatoms which are some 3 pm longer in the azaborane compound **3i**. The equivalent

Table 4 Non-hydrogen and cluster-associated hydrogen atomic coordinates ($\times 10^4$) for compounds **3i**, **4g** and **4m**, with estimated standard deviations (e.s.d.s) in parentheses

Atom	*x*	*y*	*z*	Atom	*x*	*y*	*z*
Compound **3i**							
B(1)	8 145(2)	1 518(1)	12 885(1)	H(1)	9 451(20)	903(15)	13 441(12)
B(2)	6 186(3)	2 500*	13 904(2)	H(2)	6 134(29)	2 500*	15 127(18)
B(4)	8 860(2)	2 500*	11 336(2)	H(4)	10 654(27)	2 500*	10 928(16)
B(5)	5 222(2)	1 040(1)	12 646(1)	H(5)	4 437(21)	68(18)	13 144(13)
N(6)	4 070(2)	2 500*	12 901(1)	H(6)	2 701(35)	2 500*	13 285(20)
B(9)	6 943(3)	2 500*	9 920(2)	H(9)	5 167(29)	2 500*	9 658(16)
B(10)	7 238(2)	906(1)	11 152(1)	H(10)	7 852(21)	−121(15)	10 822(12)
C(9)	8 469(2)	2 500*	8 573(1)	H(5,10)	5 222(21)	774(15)	11 225(12)
N(9)	9 632(2)	2 500*	7 612(1)	H(9a)	12 646(57)	2 500*	6 862(35)
C(91)	11 244(3)	2 500*	6 484(2)	H(9b)	11 048(34)	1 731(25)	5 906(24)
Compound **4g**							
N(1)	6 855(1)	1 677(1)	2 796(1)	B(7′)	7 508(1)	−3 696(2)	1 005(1)
N(2)	6 869(1)	−11(1)	1 837(1)	B(8′)	7 122(1)	−2 119(2)	818(1)
N(3)	8 162(1)	1 643(1)	1 936(1)	B(9′)	6 815(1)	−1 433(2)	1 764(1)
N(4)	6 250(1)	1 963(1)	1 295(1)	B(10′)	5 632(2)	−2 343(2)	1 945(1)
C(12)	6 702(1)	359(1)	2 662(1)	H(1)	6 053(15)	4 946(19)	4 661(12)
C(13)	8 006(1)	1 983(1)	2 734(1)	H(2)	6 070(15)	3 647(19)	6 175(13)
C(14)	6 066(1)	2 321(2)	2 083(1)	H(3)	4 465(15)	3 217(17)	4 649(12)
C(23)	8 027(1)	374(1)	1 816(1)	H(4)	5 373(15)	3 440(18)	3 233(12)
C(24)	6 076(1)	703(1)	1 162(1)	H(5)	8 180(16)	4 017(18)	5 691(12)
C(34)	7 362(1)	2 272(2)	1 269(1)	H(7)	5 494(16)	1 100(20)	5 603(14)
B(1)	6 303(1)	4 020(2)	4 714(1)	H(8)	4 791(14)	1 135(17)	3 707(12)
B(2)	6 252(2)	3 214(2)	5 605(1)	H(9)	7 407(13)	1 385(16)	4 132(10)
B(3)	5 279(1)	2 884(2)	4 677(1)	H(10)	7 594(13)	4 148(16)	3 806(11)
B(4)	5 882(1)	3 072(2)	3 831(1)	H(5,10)	7 993(15)	3 020(17)	4 708(12)
B(5)	7 581(2)	3 461(2)	5 297(1)	H(7,8)	6 028(16)	1 018(19)	4 603(13)
S(6)	7 369.0(3)	1 986.6(4)	5 832.7(3)	H(1′)	4 421(15)	−3 630(18)	862(12)
B(7)	5 883(2)	1 611(2)	5 236(1)	H(2′)	6 009(15)	−5 450(19)	853(12)
B(8)	5 546(1)	1 627(2)	4 088(1)	H(3′)	5 840(15)	−3 459(18)	−205(13)
B(9)	6 796(1)	1 977(2)	3 723(1)	H(4′)	5 292(14)	−1 354(17)	594(11)
B(10)	7 246(1)	3 505(2)	4 155(1)	H(5′)	5 700(17)	−4 445(19)	2 482(14)
B(1′)	5 274(1)	−3 436(2)	1 131(1)	H(7′)	8 050(15)	−4 137(17)	700(12)
B(2′)	6 248(2)	−4 536(2)	1 110(1)	H(8′)	7 355(13)	−1 566(16)	345(11)
B(3′)	6 176(2)	−3 300(2)	453(1)	H(9′)	7 491(14)	−1 702(17)	2 277(11)
B(4′)	5 806(1)	−2 018(2)	955(1)	H(10′)	5 002(16)	−1 972(18)	2 184(14)
B(5′)	6 026(2)	−3 919(2)	2 125(1)	H(5′,10′)	6 245(16)	−2 930(18)	2 549(13)
S(6′)	7 491.3(3)	−4 381.9(4)	2 079.7(3)	H(7′,8′)	7 902(16)	−2 638(19)	1 223(13)
Compound **4m**							
B(1)	2 211(1)	1 480(2)	4 059(1)	C(91)	4 080(3)	2 500*	9 562(2)
B(2)	2 716(2)	2 500*	2 805(2)	H(1)	1 413(17)	829(24)	3 955(16)
B(4)	2 551(2)	2 500*	5 385(2)	H(2)	2 209(25)	2 500*	1 927(28)
B(5)	3 571(2)	831(3)	3 443(2)	H(4)	1 911(22)	2 500*	6 129(20)
S(6)	4 433(1)	2 500*	2 727(1)	H(5)	3 626(17)	−216(26)	2 948(18)
B(9)	4 041(2)	2 500*	5 835(2)	H(9)	4 884(22)	2 500*	5 431(19)
B(10)	3 332(2)	818(2)	5 089(2)	H(10)	3 168(15)	−284(24)	5 520(17)
C(9)	4 058(2)	2 500*	7 241(2)	H(5,10)	4 215(16)	559(24)	4 473(19)
N(9)	4 078(2)	2 500*	8 268(2)				

* Parameter fixed because atom at special position.

distances and angles in **3i** are very similar to those in the related isocyanide adduct *exo*-9-(*cyclo*-$C_6H_{11}NC$)-*arachno*-6-NB_9H_{12}, which has been previously stucturally characterized.[15] Likewise, the same similarities in intracluster distances are also observed for the thiaborane analogues, **4g** and **4m**, and for the previously reported structure of *exo*-9-(NEt_3)-*arachno*-6-SB_9H_{11} **4b**,[23] although each of these three compounds has a different ligand. As also found earlier,[15,23] the most significant feature of all three structures is the asymmetry of the bonding of the H(7,8) and H(5,10) bridging hydrogen atoms, demonstrated by the shorter distances from the B(8,10) centres in all these structures. An equivalent phenomenon has also been noted and discussed for equivalent ten-vertex *arachno*-6,9-metallaheteroboranes.[36] The bis(heteroboranyl) species **4g** (Fig. 2) is of interest because it has the multidentate urotropine ligand donating to two different $\{SB_9H_{11}\}$ subclusters; comparison of equivalent interatomic distances between these two $\{arachno\text{-}6\text{-}SB_9H_{11}\}$ subclusters in this compound **4g** (see Table 5) shows no significant differences.

The ligand-to-cage C(9)–B(9) distances of *ca.* 156 pm for the two MeNC compounds **3i** and **4m** approximate to that typical for a carbon–boron two-electron two-centre single bond,[37] and the C(9)–N(9) distances of *ca.* 114 pm suggest that the essence of the triple-bond character of the MeCN ligand has been preserved in each case. The C(9)–B(9)–B(4) and H(9)–B(9)–C(9) interatomic angles [107.3(3) and 114.7(13) for **3i**, and 104.1(2) and 112.5(9)° for **4m**] suggest an approximately tetrahedral disposition of the bonding to the *exo*-ligand and the *endo*-hydrogen atom around the substituted B(9) atom, as do the corresponding angles for the urotropine compound **4g** [116.5(2) (mean) and 103.7(11)° (mean)].

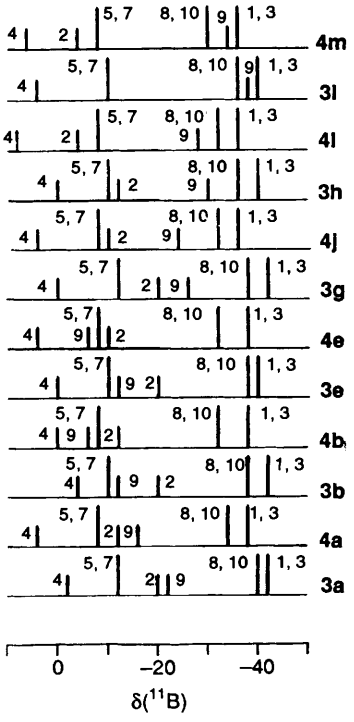

Fig. 4 Stick representations of the chemical shifts and relative intensities in the ^{11}B NMR spectra for selected pairs of isostructural compounds *exo*-9-L-*arachno*-6-NB_9H_{12} **3** and *exo*-9-L-*arachno*-6-SB_9H_{11} **4**. Not illustrated for reasons of brevity is that the individual BH(*exo*) units generate [$\delta(^1H)$, $\delta(^{11}B)$] data points (for ^1H data see Tables 8 and 9) that all fall close to a general $\delta(^1H)$ *vs.* $\delta(^{11}B)$ correlation line of slope *ca.* 1:5, intercept +2.9 in $\delta(^1H)$; most of the BH(*endo*) data points, *i.e.* those for the substituted B(9) site, are above this general correlation line (*i.e.* to higher ^1H shielding)

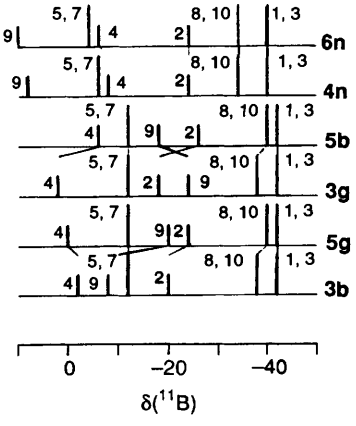

Fig. 5 Stick representations of the chemical shifts and relative intensities in the ^{11}B NMR spectra for the pairs of *exo*- and *endo*-9-L-*arachno*-6-NB_9H_{12} compounds **3b/5b** (L = NEt_3), **3g/5g** (L = CD_3CN), and *exo*- and *endo*-9-L-*arachno*-6-SB_9H_{11} compounds **4n/6n** (L = OH)

For the urotropine cage in compound **4g**, the angles about the N(1) and N(2) atoms (mean 107.9°) approximate well to an idealized tetrahedral arrangement. Attachment at the N atom of urotropine by the thiaborane moieties brings about significant lengthening of the N–C distances that involve B-substituted nitrogen atoms, the mean value being 152.0 pm in comparison with the other sets of nitrogen–carbon distances which have a mean value of 145.0 pm. This lengthening is consistent with a relatively strong electron-donating effect to the {6-SB_9H_{11}} subcluster concomitant with nitrogen quaternization. These effects are as noted for the corresponding nine-vertex *arachno* derivatives.[14] The mean B(9)–N distance of 159.7 pm in **4g** suggests a typical B–N single bond, as that in the NEt_3 analogue.[23]

Table 5 Selected interatomic distances (pm) for compounds **3i**, **4g** and **4m**

	3i[a]	**4g**	**4g**[b]	**4m**[a]
B(2)–B(1)	175.8(4)	174.8(5)	175.2(5)	175.0(4)
B(3)–B(1)	180.8(4)	181.0(5)	180.6(5)	179.4(5)
B(4)–B(1)	176.7(4)	177.8(4)	177.8(5)	176.5(4)
B(5)–B(1)	180.0(3)	177.8(5)	176.7(5)	176.5(4)
B(10)–B(1)	180.5(3)	178.9(4)	179.4(5)	179.4(3)
B(3)–B(2)	175.8(4)	175.2(5)	175.0(5)	175.0(4)
B(5)–B(2)	187.8(4)	190.5(5)	190.8(5)	189.0(4)
E(6)–B(2)	156.5(4)	194.2(4)	195.4(4)	192.6(5)
B(7)–B(2)	187.8(4)	191.5(5)	190.2(5)	189.0(4)
B(4)–B(3)	176.7(4)	177.6(4)	178.1(5)	176.5(4)
B(7)–B(3)	180.0(3)	176.5(5)	176.4(5)	176.5(4)
B(8)–B(3)	180.5(3)	179.4(4)	178.5(5)	179.4(3)
B(8)–B(4)	176.2(3)	175.3(4)	174.9(4)	175.0(4)
B(9)–B(4)	174.7(4)	172.9(4)	173.1(4)	174.2(5)
B(10)–B(4)	176.2(3)	174.8(4)	175.1(5)	175.0(4)
E(6)–B(5)	152.7(3)	192.5(4)	195.3(4)	192.9(4)
B(10)–B(5)	185.2(3)	183.6(5)	183.7(5)	184.6(5)
H(5,10)–B(5)	135.9(13)	131.8(20)	130.2(22)	137.3(21)
B(7)–E(6)	152.7(3)	194.1(4)	194.7(4)	192.9(4)
B(8)–B(7)	185.2(3)	184.4(5)	183.7(5)	184.6(5)
H(7,8)–B(7)	135.9(13)	129.6(21)	130.0(21)	137.3(21)
B(9)–B(8)	187.7(3)	188.1(4)	187.6(4)	187.2(4)
H(7,8)–B(8)	120.2(13)	114.1(22)	119.6(21)	122.5(20)
B(10)–B(9)	187.7(3)	188.6(5)	190.1(4)	187.2(4)
H(5,10)–B(10)	120.2(13)	126.3(20)	128.2(22)	122.5(20)

[a] The following atoms are related by a crystallographic mirror plane at $\frac{1}{4}$ in *b*: B(1) and B(3), B(5) and B(7) and B(10) and B(8). [b] Distances for the primed subcluster.

Mass spectrometry

The mass spectra of compounds **3a**–**3i** and **4a**–**4f** (see Tables 1 and 2) exhibit the expected molecular-ion peaks and show principal fragmentations to give $[EB_9H_{11}]^+$ (E = N or S as appropriate), this fragmentation being particularly marked for the CD_3CN and PPh_3 azaborane compounds **3g** and **3h**, where the molecular ion is not in fact observed under 70 eV electron-impact ionization conditions. This is consistent with the general trends of affinities of ligands for boron centres in polyhedral boron-containing compounds.

NMR spectroscopy

All compounds were examined by NMR spectroscopy to confirm bulk purity, and in order to measure and assign the observed resonances and to define the shielding properties induced by the individual Lewis bases L. Boron-11 and ^1H NMR spectroscopy, making use of the [^{11}B–^{11}B] COSY[39] (for characteristic cross-peaks see Tables 8 and 9) and ^1H-{^{11}B(selective)} techniques,[40] resulted in the complete assignment of all the ^1H and ^{11}B resonances for all the compounds **3a**–**3i** and **4a**–**4n**. The measured data for these series of new ten-vertex *arachno* azaboranes and thiaboranes are in Tables 8 and 9 respectively, and illustrative aspects of the ^{11}B shielding behaviour for selected compounds are presented graphically in Figs. 4 and 5.

The NMR data for all the azaborane compounds **3a**–**3i** and the thiaborane compounds **4a**–**4n** are entirely consistent with the general constitutions as represented schematically and also with the results of the X-ray diffraction studies (Figs. 1–3) and mass spectrometry. Intercomparison of the ^{11}B shielding patterns among both sets of compounds **3** and **4** (Fig. 4) reveals similar shielding behaviour for all the compounds.

It is readily seen (see also Tables 8 and 9) that the principal

Table 6 Selected cluster bond angles (°) for compounds **3i**, **4g** and **4m**

	3i[a]	4g	4g[b]	4m[a]
B(3)–B(1)–B(2)	59.1(2)	59.0(2)	58.9(2)	59.2(2)
B(4)–B(1)–B(2)	110.3(2)	108.8(2)	108.9(2)	109.5(2)
B(4)–B(1)–B(3)	59.3(2)	59.3(2)	59.6(2)	59.5(2)
B(5)–B(1)–B(2)	63.7(2)	65.4(2)	65.7(2)	65.1(2)
B(5)–B(1)–B(3)	104.2(2)	108.7(2)	109.3(2)	108.9(2)
B(5)–B(1)–B(4)	104.8(2)	106.3(2)	106.8(2)	107.5(2)
B(10)–B(1)–B(2)	117.3(2)	116.6(2)	116.7(2)	116.5(2)
B(10)–B(1)–B(3)	108.2(2)	109.2(2)	109.4(2)	108.8(2)
B(10)–B(1)–B(4)	59.1(2)	58.7(2)	58.7(2)	58.9(2)
B(10)–B(1)–B(5)	61.8(2)	62.0(2)	62.1(2)	62.5(2)
B(3)–B(2)–B(1)	61.9(2)	62.3(2)	62.1(2)	61.7(2)
B(5)–B(2)–B(1)	59.2(2)	58.1(2)	57.5(2)	57.9(2)
B(5)–B(2)–B(3)	103.0(2)	105.6(2)	105.6(2)	105.3(2)
E(6)–B(2)–B(1)	101.6(2)	110.3(2)	110.4(2)	111.0(2)
E(6)–B(2)–B(3)	101.6(2)	109.8(2)	110.3(2)	111.0(2)
E(6)–B(2)–B(5)	51.7(2)	60.0(2)	60.7(2)	60.7(2)
B(7)–B(2)–B(1)	103.0(2)	105.8(2)	105.7(2)	105.3(2)
B(5)–B(2)–B(3)	59.2(2)	57.4(2)	57.6(2)	57.9(2)
B(7)–B(2)–B(5)	103.0(2)	102.2(2)	102.7(2)	101.9(2)
B(7)–B(2)–E(6)	51.7(2)	60.4(2)	60.6(2)	60.7(2)
B(2)–B(3)–B(1)	59.1(2)	58.8(2)	59.0(2)	59.2(2)
B(4)–B(3)–B(1)	59.3(2)	59.4(2)	59.4(2)	59.5(2)
B(4)–B(3)–B(2)	110.3(2)	108.7(2)	108.8(2)	109.5(2)
B(7)–B(3)–B(1)	104.2(2)	109.7(2)	109.4(2)	108.9(2)
B(7)–B(3)–B(2)	63.7(2)	66.0(2)	65.5(2)	65.1(2)
B(7)–B(3)–B(4)	104.8(2)	107.1(2)	107.0(2)	107.5(2)
B(8)–B(3)–B(1)	108.2(2)	109.6(2)	109.3(2)	108.8(2)
B(8)–B(3)–B(2)	117.3(2)	117.1(2)	116.7(2)	116.5(2)
B(8)–B(3)–B(4)	59.1(2)	58.8(2)	58.7(2)	58.9(2)
B(8)–B(3)–B(7)	61.8(2)	62.4(2)	62.3(2)	62.5(2)
B(3)–B(4)–B(1)	61.5(2)	61.2(2)	61.0(2)	61.1(2)
B(8)–B(4)–B(1)	112.0(2)	113.0(2)	112.3(2)	112.4(2)
B(8)–B(4)–B(3)	61.5(2)	61.1(2)	60.7(2)	61.4(2)
B(9)–B(4)–B(1)	118.1(2)	116.1(2)	116.5(2)	116.4(2)
B(9)–B(4)–B(3)	118.1(2)	115.7(2)	115.8(2)	116.4(2)
B(9)–B(4)–B(8)	64.7(2)	65.4(2)	65.2(2)	64.8(2)
B(10)–B(4)–B(1)	61.5(2)	61.0(2)	61.1(2)	61.4(2)
B(10)–B(4)–B(3)	112.0(2)	112.6(2)	112.6(2)	112.4(2)
B(10)–B(4)–B(8)		117.7(2)	117.5(2)	115.4(2)
B(10)–B(4)–B(9)	64.7(2)	65.7(2)	66.2(2)	64.8(2)
B(2)–B(5)–B(1)	57.1(2)	56.5(2)	56.8(2)	57.1(2)
E(6)–B(5)–B(1)	101.3(2)	109.7(2)	109.8(2)	110.2(2)
E(6)–B(5)–B(2)	53.6(2)	60.9(2)	60.8(2)	60.6(2)
B(10)–B(5)–B(1)	59.2(2)	59.3(2)	59.7(2)	59.6(2)
B(10)–B(5)–B(2)	109.3(2)	107.1(2)	107.4(2)	107.6(2)
B(10)–B(5)–E(6)	117.9(2)	118.5(2)	118.1(2)	119.0(2)
B(5)–E(6)–B(2)	74.8(2)	59.0(2)	58.5(2)	58.7(2)
B(7)–E(6)–B(2)	74.8(2)	59.1(2)	58.4(2)	58.7(2)
B(7)–E(6)–B(5)	123.4(2)	100.5(2)	99.5(2)	99.1(2)
B(3)–B(7)–B(2)	57.1(2)	56.7(2)	56.9(2)	57.1(2)
E(6)–B(7)–B(2)	53.6(2)	60.5(2)	61.0(2)	60.6(2)
E(6)–B(7)–B(3)	101.3(2)	109.2(2)	110.0(2)	110.2(2)
B(8)–B(7)–B(2)	109.3(2)	107.1(2)	107.2(2)	107.6(2)
B(8)–B(7)–B(3)	59.2(2)	59.5(2)	59.4(2)	59.6(2)
B(8)–B(7)–E(6)	117.9(2)	117.7(2)	118.0(2)	119.0(2)
B(4)–B(8)–B(3)	59.4(2)	60.1(2)	60.5(2)	60.1(2)
B(7)–B(8)–B(3)	58.0(2)	58.0(2)	58.3(2)	58.0(2)
B(7)–B(8)–B(4)	102.9(2)	104.7(2)	105.2(2)	104.7(2)
B(9)–B(8)–B(3)	107.8(2)	107.8(2)	108.7(2)	108.8(2)
B(9)–B(8)–B(4)	57.3(2)	56.7(2)	56.9(2)	57.4(2)
B(9)–B(8)–B(7)	111.0(2)	110.0(2)	110.8(2)	111.8(2)
B(8)–B(9)–B(4)	58.0(2)	57.9(2)	57.8(2)	57.8(2)
B(10)–B(9)–B(4)	58.0(2)	57.6(2)	57.4(2)	57.8(2)
B(10)–B(9)–B(8)	102.8(2)	105.4(2)	104.8(2)	104.4(2)
B(4)–B(10)–B(1)	60.4(2)	60.4(2)	60.2(2)	60.4(2)
B(5)–B(10)–B(1)	59.0(2)	58.7(2)	58.2(2)	58.0(2)
B(5)–B(10)–B(4)	102.9(2)	105.1(2)	104.9(2)	104.7(2)
B(9)–B(10)–B(1)	109.9(2)	108.1(2)	107.7(2)	108.8(2)
B(9)–B(10)–B(4)	57.3(2)	56.7(2)	56.4(2)	57.4(2)
B(9)–B(10)–B(5)	111.0(2)	109.6(2)	110.2(2)	111.8(2)

[a] The following atoms are related by a crystallographic mirror plane at $\frac{1}{4}$ in *b*: B(1) and B(3), B(5) and B(7) and B(10) and B(8). [b] Angles for the primed subcluster.

Table 7 Selected exocluster bond distances (pm) and angles (°) for compounds **3i**, **4g** and **4m**

Compound **3i**			
H(6)–N(6)	88.9(21)	C(9)–B(9)	155.9(4)
N(9)–C(9)	113.9(3)	C(91)–N(9)	143.1(3)
N(9)–C(9)–B(9)	178.2(2)	C(91)–N(9)–C(9)	175.4(2)
Compound **4g**			
C(12)–N(1)	149.7(3)	C(12)–N(2)	149.8(3)
C(13)–N(1)	153.1(4)	C(23)–N(2)	154.2(4)
C(14)–N(1)	152.3(4)	C(24)–N(2)	152.8(4)
B(9)–N(1)	159.7(4)	B(9′)–N(2)	159.6(4)
C(13)–N(1)–C(12)	107.5(2)	C(23)–N(2)–C(12)	107.6(2)
C(14)–N(1)–C(12)	108.4(2)	C(24)–N(2)–C(12)	107.8(2)
C(14)–N(1)–C(13)	107.1(2)	C(24)–N(2)–C(23)	107.0(2)
B(9)–N(1)–C(12)	108.3(2)	B(9′)–N(2)–C(12)	109.3(2)
Compound **4m**			
N(9)–C(9)	113.9(4)	C(9)–B(9)	156.0(5)
C(91)–N(9)	143.6(4)		
N(9)–C(9)–B(9)	179.6(2)	C(91)–N(9)–C(9)	178.9(2)

significant differences are among the ligand-substituted B(9) sites, with ligand-induced ^{11}B shielding increasing in the series: *endo*-OH^- < *exo*-OH^- ≪ NEt_3 < pyridine, isoquinoline < quinoline < urotropine < $\frac{1}{2}$ urotropine < NH_3 < SMe_2 < H^- < NC^- < MeCN < PPh_3 < MeNC. The same order of ^{11}B shielding induced by individual ligands at the substituted site has also been observed in the two series of nine-vertex compounds that consist of the corresponding nine-vertex thiaboranes *exo*-6-L-*arachno*-4-SB_8H_{10} **9** and the corresponding carbaboranes *exo*-6-L-*arachno*-4-CB_8H_{12}.[14,41] The corresponding nine-vertex azaboranes *exo*-6-L-*arachno*-4-NB_8H_{11} also appear to show similar trends.[7] The ^{11}B(9) shielding for the {CN^-} compound **4k** approximates to that for the MeCN derivative **4j** rather than to that for the MeNC derivative **4m**. This introduces the possibility that **4k** may have an isocyano-arrangement, involving an N–B(9) bond, rather than the C–B(9) cyano-constitution previously suggested,[27] although this is tentative because structurally correlated comparison NMR data are not available.

An approximately reverse ordering of ligand-induced shieldings in both series of compounds **3** and **4** can be observed at the B(2) site, *i.e.* the site antipodal to the substituted B(9) site. A preliminary account of the quantitative assessment of both of these effects has been reported[42] and will be discussed in more detail in a separate paper. Other long-range substituent effects are very small, and there are only trivial differences in chemical shift, and (sometimes) in the corresponding ordering among closely spaced resonances, for the other sites. The individual $\delta(^{11}B)$, $\delta(^1H)$ data points for all the azaborane and thiaborane compounds **3** and **4** are close to a single $\delta(^{11}B)$ *vs.* $\delta(^1H)$ correlation line (see notes to Fig. 4), except for the more highly shielded ^{1}H(*endo*-9) positions. This is as found also for the nine-vertex thiaborane compounds of structure **9** and their carbaborane analogues,[14,19,41,42] and for H(*endo*) shieldings in general.[43] Fig. 5 shows a graphical correlation of the ^{11}B chemical shifts for individual pairs of *exo* and *endo* derivatives of structure types **3**/**5** and **4**/**6**. It can be seen that the shielding patterns within each of the three pairs of isomeric compounds is quite similar. The differences occur at the *exo*/*endo* ligand-substituted B(9) site, which may be expected, but there are also changes at the B(8,10) and B(4) sites adjacent to the substituted site, and a significant antipodal change at B(2).

Table 8 Boron-11 and ^1H chemical shifts for the compounds *exo*-9-L-*arachno*-6-NB_9H_{12} **3** and *endo*-9-L-*arachno*-6-NB_9H_{12} **5** at 294–297 K

$\delta(^{11}B)$,[a] $^1J(^{11}B-^1H)$ in parentheses, $\delta(^1H)$[a] in square brackets

Compound	Ligand	BH(4)	BH(2)	BH(5,7)	BH(9)[b]	BH(8,10)	BH(1,3)	μ-H
3a	H[c,d]	−0.1 (133) [2.52]	−19.9 (164) [1.90]	−12.0 (141) [2.27]	−21.5 (115)[e] [1.50][f,g] [0.74]	−40.4 (—)[f] [0.38]	−41.2 (140)[f] [0.54]	— — [−2.28]
3b	NEt_3[c]	−2.9 (132) [2.79]	−20.2 (166) [2.08]	−11.6 (144) [2.40]	−8.9 (134) [2.45]	−38.2 (138/58) [0.43]	−42.1 (142) [0.31]	— — [−2.39]
5b	*endo*-NEt_3[c]	−1.0	−23.2	−11.6	−19.5	−41.1	−41.8	—
3c	quin[c]	+2.8 (146) [2.97]	−19.2 (166) [2.22]	−11.3 (160)[f] [2.61]	−12.5 (130) [2.52]	−37.6 (130/60)[f] [0.70]	−41.3 (140)[f] [0.54]	— — [−1.91]
3d	iquin[c]	+2.5 (142) [2.91]	−18.9 (165) [2.19]	−11.4 (140)[f] [2.55]	−10.8 (—)[f] [2.43]	−38.2 (125/55)[f] [0.71]	−41.4 (141) [0.46]	— — [−2.05]
3e	py[c]	+2.7 (136) [2.78]	−18.8 (167) [2.16]	−11.4 (125)[f] [2.50]	−12.1 (125)[f] [2.30]	−37.7 (128/57) [0.61]	−40.0 (143) [0.46]	— — [−2.15]
3f	uro[h]	−2.8 (125) [2.53]	−19.3 (147) [1.90]	−11.3 (—)[f] [2.25]	−11.5 (—)[f] [0.55]	−39.5 (146/50)[f] [0.33]	−41.5 (140) [0.14]	— — [−2.61]
3g	CD_3CN[h,i]	+2.2 (135) [2.78]	−18.2 (163) [1.91]	−12.2 (145)[f] [2.27]	−24.4 (—)[f] [1.29]	−37.8 (140/52) [0.44]	−41.4 (142) [0.25]	— — [−2.49]
5g	*endo*-CD_3CN[h,j]	−5.5	−26.1	−12.2[f]	−18.2[f]	−40.6	−42.8	
3h	PPh_3[c]	+3.3 (138) [2.90]	−13.4 (158) [2.31]	−11.5 (137)[k] [2.51]	−28.8 (—)[f,k] [1.26]	−36.5 (143) [0.57]	−40.0 (144) [0.43]	— — [−1.80]
3i	MeNC[c]	+5.3 (140) [3.06]	−12.0 (147)[f] [2.31]	−12.0 (147)[f] [2.42]	−38.5 (127) [0.45]	−35.6 (145/36) [0.64]	−39.9 (144) [0.53]	— — [−2.14]

[a] Assignment by relative intensities, [$^{11}B-^{11}B$] COSY (measured for all compounds, typical observed cross-peaks: 1,3–2s; 1,3–4s; 1,3–5,7s; 1,3–8,10s; 2–5,7w–?; 8,10–9s; s = strong, w = weak, ? = uncertain), [$^1H-^1H$] COSY (measured for compounds **3c** and **3e**, typical observed cross-peaks: 1,3–2m; 1,3–4s; 1,3–5,7m; 1,3–8,10s; 1,3-μ-5,10/7,8s; 2–5,7w; μ-5,10/7,8–9m) and $^1H-\{^{11}B(selective)\}$ experiments (for ^1H). Additionally $\delta(^1H)$ (NH) for all compounds observed between +2.5 and +3.0; some variation of δ with solution conditions. [b] Signals of the *endo* hydrogen atoms. Additional signals of the exoskeletal ligand: **3b**, δ 1.34 (t, 3 H, NEt_3), 3.11 (q, 2 H, NEt_3); **3c**, 9.0–7.3 (m, 7 H, quin); **3d**, 9.48–7.8 (m, 7 H, iquin); **3e**, 8.81–7.25 (m, 5 H, py); **3f**, 4.79–4.17 (m, 12 H, uro); **3h**, *ca.* 7.55 (centre) (m, 15 H, PPh_3); **3i**, 3.57 (s, 3, MeNC). [c] In $CDCl_3$. [d] $[NBu_4]^+$ salt. [e] Triplet due to the $\{BH_2\}$ group. [f] Value uncertain, usually due to peak overlap. [g] *exo*-Hydrogen. [h] In CD_3CN. [i] In $(CD_3)_2CO$. [j] $[NMe_4]^+$ salt. [k] $^1J(^{11}B-^{31}P)$ *ca.* 105 Hz.

Table 9 Boron-11 and ^1H chemical shifts for *exo*-9-L-*arachno*-6-SB_9H_{11} compounds **4** at 294–297 K

$\delta(^{11}B)$,[a] $^1J(^{11}B-^1H)$ in parentheses, $\delta(^1H)$[a] in square brackets

Compound	Ligand	BH(4)	BH(2)	BH(5,7)	BH(9)[b]	BH(8,10)	BH(1,3)	μ-5,7/8,10
4a	H[c,d]	3.6 (131) [2.78]	−11.6 (159) [2.45]	−8.4 (147) [2.47]	−16.1 (113)[e] [1.33][f] [0.46]	−33.9 (134) [0.38]	−37.1 (137) [0.74]	— — [−1.81]
4b	NEt_3[c]	1.6 (140) [2.91]	−11.4 (172) [2.60]	−8.4 (155) [2.59]	−5.4 (128) [0.63]	−32.3 (144/39) [0.82]	−38.1 (154) [0.86]	— — [−1.32]
4c	quin[c]	6.4 (137) [3.11]	−10.8 (173) [2.65]	−8.1 (165)[g] [2.72]	−8.1 (—)[g] [2.25]	−31.2 (147/40) [1.05]	−37.0 (147) [1.05]	— — [−1.48]
4d	iquin[c]	5.8 (136) [3.03]	−11.0 (170) [2.65]	−8.4 (163)[g] [2.67]	−6.8 (120)[g] [2.14]	−31.2 (147/40) [1.05]	−37.0 (147) [1.05]	— — [−1.57]

Table 9 (*continued*)

Compound	Ligand	$\delta(^{11}B)$,[a] $^1J(^{11}B-^1H)$ in parentheses, $\delta(^1H)$[a] in square brackets						
		BH(4)	BH(2)	BH(5,7)	BH(9)[b]	BH(8,10)	BH(1,3)	μ-5,7/8,10
4e	py[c]	+5.9 (134) [3.04]	−10.6 (170)[g] [2.57]	−8.4 (145)[g] [2.56]	−7.4 (120)[g] [2.04]	−31.4 (144/48) [0.96]	−37.2 (147) [0.93]	— — [−1.65]
4f	uro[c]	+2.4 (131) [2.87]	−8.1 (—)[g] [2.72]	−8.1 (—)[g] [2.63]	−9.8 (—)[g] [0.39]	−33.6 (146/50) [0.87]	−37.5 (148) [1.00]	— — [−2.24]
4g	½uro[h]	+2.4 (134) [2.81]	−8.1 (—)[g] [2.50]	−8.1 (—)[g] [2.50]	−9.6 (—)[g] [0.45]	−32.7 (144/47) [0.86]	−37.4 (144) [0.80]	— — [−2.08]
4h	NH_3[h]	+5.2 (134) [2.69]	−12.0 (—)[g] [2.49]	−7.7 (153) [2.42]	−12.5 (—)[g] [1.04]	−32.0 (147/40) [0.69]	−37.4 (146) [0.75]	— — [−1.99]
4i	SMe_2[i]	+7.3 (139) [3.01]	−7.4 (146)[g] [2.61]	−7.5 (146)[g] [2.61]	−13.1 (137) [1.17]	−31.4 (141/35) [0.88]	−36.0 (146) [0.99]	— — [−1.85]
4j	MeCN[c]	+7.0 (132) [2.98]	−9.8 (146)[g] [2.55]	−8.5 (146)[g] [2.51]	−21.1 (122) [1.02]	−30.6 (163) [0.85]	−36.9 (144) [0.88]	— — [−2.09]
4k	NC^-[h,j]	+8.3 (140) [2.94]	−7.9 (147)[g] [2.74]	−6.9 (135)[g] [2.61]	−19.5 (122) [1.91]	−30.7 (147) [0.73]	−34.5 (144) [0.95]	— — [−2.08]
4l	PPh_3[c]	+7.4 (141) [2.96]	−4.5 (—)[k] [2.88]	−7.8 (150) [2.71]	−25.5 (116)[f,l] [1.02]	−31.3 (151/50) [0.96]	−36.5 (150) [1.04]	— — [−1.52]
4m	MeNC[c]	+8.7 (140) [3.11]	−3.1 (177) [2.87]	−8.6 (155) [2.62]	−34.6 (111) [0.19]	−29.4 (149/37) [1.05]	−35.6 (143) [1.08]	— — [−1.85]
4n	OH^-[h,m]	−7.2 (128) [1.95][g]	−23.3 (165) [1.81][g]	−5.2 (149) [2.55]	7.2 (128) [1.95][g]	−34.0 (134) [0.43]	−38.9 (140) [0.47]	— — [−1.75]
6n	*endo*-OH^-[h,m]	−6.2 (132) [1.86][f]	−24.3 (168) [1.75]	−4.6 (149) [2.58]	8.6 (125) [2.18]	−33.7 (135/35) [0.43]	−38.7 (140) [0.48]	— — [−1.67]

[a] Assignment by relative intensities, [$^{11}B-^{11}B$] COSY (measured for all compounds, typical observed cross-peaks: 1,3–2s; 1,3–4s; 1.3–5,7s; 1.3–8,10s; 2–5,7w–?,8,10–9s) and $^1H-\{^{11}B$(selective)$\}$ experiments (for ^1H). [b] Signals of the *endo*-hydrogen atoms. Additional signals of the exoskeletal ligand: **4b**, δ 3.11 (q, 2 H, NEt_3), 1.30 (t, 3 H, NEt_3); **4c**, 9.0–7.25 (m, 7 H, quin); **4d**, 9.50–7.70 (m, 7 H, iquin); **4e**, 8.97–7.70 (m, 5 H, py); **4f**, 4.95–4.68 (m, 12 H, uro); **4g**, 4.87–4.46 (m, 12 H, uro); **4h**, NH_3 protons not observed; **4i**, 2.69 (s, 6 H, SMe_2); **4j**, 2.10 (s, 3 H, MeCN); **4l**, *ca.* 7.65 (centre) (m, 15 H, PPh_3); **4m**, 3.62 (s, 3 H, MeNC); **4n**, 3.57 (q, 1 H, OH^-); **6n**, 4.02 (m, 1 H, OH^-). [c] In $CDCl_3$. [d] $[NBu_4]^+$ salt. [e] Triplet due to the $\{BH_2\}$ group. [f] *exo*-Hydrogen. [g] Value uncertain, usually due to peak overlap. [h] In CD_3CN. [i] In $(CD_3)_2CO$. [j] $[NMe_4]^+$ salt. [k] Broad signal, $^1J(^{11}B-^1H)$ cannot be defined. [l] $^1J(^{11}B-^{31}P) = 104$ Hz. [m] $[PPh_4]^+$ salt.

Acknowledgements

Contribution No. 58 from the Řež–Leeds Anglo–Czech Polyhedral Collaboration (A.C.P.C.). The authors thank the Academy of Sciences of the Czech Republic (Grants no. 43203 and 43204), the UK SERC (Grants no. F43215 and F78323), the Royal Society (London, UK) and Borax Research Ltd. (Chessington, UK) for support (to B. S., J. H. and T. J.), and Drs. T. S. Griffin, R. A. Walker and D. M. Wagnerová and Professor N. N. Greenwood for their helpful interest. We also thank Dr. Z. Weidenhoffer and Mr. D. Singh for mass spectrometric measurements.

References

1 B. Štíbr, J. Plešek and S. Heřmánek, in *Advances in Boron and the Boranes*, eds. J. E. Liebman, A. Greenberg and R. E. Williams, VCH, New York, 1988, pp. 35–70 and refs. therein.

2 K. Baše, J. Plešek, S. Heřmánek, J. Huffman, P. Ragatz and R. Schaeffer, *J. Chem. Soc., Chem. Commun.*, 1975, 934.

3 K. Baše, F. Hanousek, B. Štíbr, J. Plešek and J. Lyčka, *J. Chem. Soc., Chem. Commun.*, 1981, 1162.

4 K. Baše, *Collect. Czech. Chem. Commun.*, 1983, **48**, 2593.

5 B. Štíbr, J. D. Kennedy and T. Jelínek, *J. Chem. Soc., Chem. Commun.*, 1990, 1309.

6 T. Jelínek, J. D. Kennedy and B. Štíbr, *J. Chem. Soc., Chem. Commun.*, 1994, 677.

7 T. Jelínek, J. D. Kennedy and B. Štíbr, *Collect. Czech. Chem. Commun.*, 1994, **59**, 2244.

8 K. Baše, V. Gregor and S. Heřmánek, *Chem. Ind. (London)*, 1979, 743.

9 K. Baše, X. L. R. Fontaine, N. N. Greenwood, J. H. Jones, J. D. Kennedy, B. Štíbr and M. G. H. Wallbridge, *Polyhedron*, 1989, **8**, 2089.

10 M. Bown, X. L. R. Fontaine and J. D. Kennedy, *J. Chem. Soc., Dalton Trans.*, 1988, 1468.

11 K. Nestor, X. L. R. Fontaine, N. N. Greenwood, J. D. Kennedy and M. Thornton-Pett, *J. Chem. Soc., Dalton Trans.*, 1991, 2657.

12 T. Jelínek, B. Štibr, J. D. Kennedy and M. Thornton-Pett, *Angew. Chem., Int. Edn. Engl.*, 1994, **33**, 1599.
13 T. Jelínek, J. D. Kennedy and B. Štíbr, *J. Chem. Soc., Chem. Commun.*, 1994, 1415; P. Kaur, J. Holub, N. P. Rath, J. Bould, L. Barton, B. Štibr and J. D. Kennedy, *Chem. Commun.*, 1996, 273.
14 J. Holub, B. Štíbr, J. D. Kennedy, M. Thornton-Pett, T. Jelínek and J. Plešek, *Inorg. Chem.*, 1994, **33**, 4545.
15 A. Arafat, J. Baer, J. C. Huffman and L. J. Todd, *Inorg. Chem.*, 1986, **25**, 3757.
16 J. G. Kester, J. C. Huffman and L. J. Todd, *Inorg. Chem.*, 1988, **25**, 4528.
17 W. R. Hertler, F. Klanberg and E. L. Muetterties, *Inorg. Chem.*, 1967, **6**, 1696.
18 W. R. Pretzer and R. W. Rudolph, *J. Am. Chem. Soc.*, 1976, **98**, 1441.
19 R. W. Rudolph and W. R. Pretzer, *Inorg. Synth.*, 1983, **22**, 226.
20 V. V. Volkov, E. A. Il'inchik, E. A. Volkov and O. V. Voronina, *Izv. Akad. Nauk SSSR, Ser. Khim.*, 1990, 2113.
21 F. Klanberg, E. L. Muetterties and L. J. Guggenberger, *Inorg. Chem.*, 1968, **7**, 2272.
22 A. R. Siedle, G. M. Bodner, A. R. Garber and L. J. Todd, *Inorg. Chem.*, 1974, **13**, 1756.
23 T. K. Hilty and R. W. Rudolph, *Inorg. Chem.*, 1979, **18**, 1106.
24 S. Küpper and L. G. Sneddon, *J. Am. Chem. Soc.*, 1992, **114**, 4914.
25 S. Küpper, P. J. Carroll and L. G. Sneddon, *Inorg. Chem.*, 1992, **31**, 4921.
26 A. R. Siedle, D. McDowell and L. J. Todd, *Inorg. Chem.*, 1974, **13**, 2735.
27 A. Arafat, G. D. Friesen and L. J. Todd, *Inorg. Chem.*, 1983, **25**, 3721.
28 J. Casanova, jun., R. E. Schuster and N. D. Werner, *J. Chem. Soc.*, 1963, 4280.
29 J. Plešek, B. Štíbr, X. L. R. Fontaine, J. D. Kennedy, S. Heřmánek and T. Jelínek, *Collect. Czech. Chem. Commun.*, 1991, **56**, 1618.
30 J. D. Kennedy, X. L. R. Fontaine, M. McGrath and T. R. Spalding, *Magn. Reson. Chem.*, 1991, **29**, 711.
31 W. McFarlane, *Proc. R. Soc. London, Ser. A*, 1986, **306**, 185.
32 W. Clegg, *Acta Crystallogr., Sect. A*, 1981, **37**, 22.
33 G. M. Sheldrick, *Acta Crystallogr., Sect. A*, 1990, **46**, 467.
34 G. M. Sheldrick, SHELX 76, Program System for X-Ray Structure Determinations, University of Cambridge, 1976.
35 C. K. Johnson, ORTEP, Report ORNL-5138, Oak Ridge National Laboratory, Oak Ridge, TN, 1976.
36 Faridoon, T. R. Spalding, O. Ni Dhubhghaill, G. Ferguson, X. L. R. Fontaine and J. D. Kennedy, *J. Chem. Soc., Dalton Trans.*, 1989, 1657.
37 M. Elian and R. Hoffman, *Inorg. Chem.*, 1975, **14**, 1058; R. Hoffman, *Science (Washington D. C.)*, 1981, **211**, 995.
38 R. A. Beaudet, in *Advances in Boron and the Boranes*, eds. J. E. Liebman, A. Greenberg and R. E. Williams, VCH, New York, 1988, ch. 20, pp. 417–490 and refs. therein.
39 W. C. Hutton, T. L. Venable and R. N. Grimes, *J. Am. Chem. Soc.*, 1984, **106**, 29.
40 X. L. R. Fontaine and J. D. Kennedy, *J. Chem. Soc., Dalton Trans.*, 1987, 1573.
41 J. Plešek, B. Štíbr, T. Jelínek, X. L. R. Fontaine, M. Thornton-Pett, S. Heřmánek and J. D. Kennedy, *Inorg. Chem.*, 1994, **33**, 2994.
42 B. Štíbr and J. D. Kennedy, *Proceedings of the 8th International Meeting on Boron Chemistry*, Knoxville, Tennessee 11–15 July, 1993, Abstract PN-26, p. 108.
43 See, for example, J. D. Kennedy, in *Multinuclear NMR*, ed. J. Mason, Plenum, London and New York, 1987, pp. 221–254 and refs. therein.

Received 12*th September* 1995; *Paper* 5/06033H